






Polysaccharide oxidation by lytic polysaccharide monoxygenase is enhanced by engineered cellobiose dehydrogenase

Daniel Kracher^{1,2} , Zarah Forsberg³ , Bastien Bissaro³ , Sonja Gangl¹, Marita Preims¹, Christoph Sygmund¹, Vincent G. H. Eijsink³  and Roland Ludwig¹ 

1 Department of Food Science and Technology, BOKU – University of Natural Resources and Life Sciences, Vienna, Austria

2 Manchester Institute of Biotechnology, The University of Manchester, Manchester, UK

3 Faculty of Chemistry, Biotechnology and Food Science, Norwegian University of Life Sciences (NMBU), Ås, Norway

Keywords

cellobiose dehydrogenase; cellulose degradation; copper monoxygenase; hydrogen peroxide; lytic polysaccharide monoxygenase

Correspondence

R. Ludwig, Department of Food Sciences and Technology, BOKU – University of Natural Resources and Life Sciences, Vienna 1190, Austria

Tel: +431 47654 75216

E-mail: roland.ludwig@boku.ac.at

and

V. G. H. Eijsink, Faculty of Chemistry, Biotechnology and Food Science, Norwegian University of Life Sciences (NMBU), 1432 Ås, Norway

Tel.: +4767232463

E-mail: vincent.eijsink@nmbu.no

Daniel Kracher and Zarah Forsberg contributed equally to this article

(Received 21 June 2019, revised 13 August 2019, accepted 16 September 2019)

doi:10.1111/febs.15067

The catalytic function of lytic polysaccharide monoxygenases (LPMOs) to cleave and decrystallize recalcitrant polysaccharides put these enzymes in the spotlight of fundamental and applied research. Here we demonstrate that the demand of LPMO for an electron donor and an oxygen species as cosubstrate can be fulfilled by a single auxiliary enzyme: an engineered fungal cellobiose dehydrogenase (CDH) with increased oxidase activity. The engineered CDH was about 30 times more efficient in driving the LPMO reaction due to its 27 time increased production of H₂O₂ acting as a cosubstrate for LPMO. Transient kinetic measurements confirmed that intra- and intermolecular electron transfer rates of the engineered CDH were similar to the wild-type CDH, meaning that the mutations had not compromised CDH's role as an electron donor. These results support the notion of H₂O₂-driven LPMO activity and shed new light on the role of CDH in activating LPMOs. Importantly, the results also demonstrate that the use of the engineered CDH results in fast and steady LPMO reactions with CDH-generated H₂O₂ as a cosubstrate, which may provide new opportunities to employ LPMOs in biomass hydrolysis to generate fuels and chemicals.

Introduction

Lytic polysaccharide monoxygenases (LPMOs, EC: 1.14.99.53-56, CAZy IDs: AA9-11, AA13-16) are copper-containing enzymes found in chitin-, starch-, and plant cell wall-degrading organisms [1–5]. LPMOs use an unprecedented oxidative reaction mechanism to

cleave and locally decrystallize these biopolymers, which enhances the activity of associated hydrolases [1,2,6–8]. The reaction cycle starts with the reduction of LPMO's mononuclear type-II copper by external electron donors. After binding of a cosubstrate (O₂ or

Abbreviations

AsCA, ascorbic acid; CDH, cellobiose dehydrogenase; CYT, cytochrome domain of CDH; DH, dehydrogenase domain of CDH; FAD, flavin adenine dinucleotide; LPMO, lytic polysaccharide monoxygenase.

H₂O₂), an oxygen atom is inserted into the C–H bond at the C1 or C4 carbon of a glycosidic bond in the substrate [9–11], which is broken by a spontaneous elimination reaction. The detailed catalytic mechanism of LPMOs and the nature of their cosubstrate are currently debated. Both O₂ [12–14] and H₂O₂ [15,16] are reported to interact with reduced LPMO, but with different implications on the reaction pathway. The monooxygenase reaction using O₂ requires two sequential electron transfer steps and is likely to proceed via an intermittent dioxo [9,12] or oxyl [17] species. In contrast, a single reduction step to yield Cu(I) could be followed by binding of H₂O₂ to directly form an oxyl- or a hydroxyl species [15]. The reported turnover numbers of LPMO with H₂O₂ as cosubstrate are one to two orders of magnitude higher than those reported with O₂ depending on the substrate and reaction conditions [15,16,18]. However, exceeding H₂O₂ concentrations also lead to enzyme inactivation via autooxidation of, primarily, the Cu-coordinating histidine residues [15]. This makes a controlled supply of H₂O₂ essential to maintain LPMO stability during catalysis [16,19].

In lignocellulose-degrading fungi, one known route for LPMO reduction involves the electron transfer protein cellobiose dehydrogenase (CDH; EC: 1.1.99.18; CAZy ID: AA3_1) [6,11,20]. CDHs are widely distributed extracellular flavocytochromes comprising a flavin adenine dinucleotide (FAD)-containing dehydrogenase domain (DH) for substrate oxidation that transfers electrons to a mobile cytochrome *b* domain that can reduce the LPMO active site [9,11,20,21]. CDHs have a reported low oxidase activity [22–25], for example, the *Crassiacarpon hotsonii* (syn. *Myriococcum thermophilum*) CDH (*ChCDH*) used in this study has a ca. 200 times lower turnover number for O₂ than for flavin-dependent 1,4-benzoquinone reduction [26]. Still, under physiological conditions, CDH might provide catalytically relevant amounts of H₂O₂ for LPMOs, which have a μM affinity for this cosubstrate [16,27]. To scrutinize the significance of H₂O₂ in CDH-driven LPMO activity, we enhanced the H₂O₂ production rate of *ChCDH* by means of genetic engineering. Our results demonstrate that a single synthetic enzyme, hereafter termed CDH_{oxy+}, is able to fulfill a dual function as LPMO reductase and as a supplier of H₂O₂ for the LPMO reaction. This allowed reducing the effective concentration of CDH during oxidative polysaccharide degradation by a factor of ~30 relative to the wild-type *ChCDH*, while achieving similar LPMO activity. The results shed light on the role of H₂O₂ in LPMO catalysis and the CDH-LPMO interplay.

Results and Discussion

Engineering of *ChCDH* for increased oxygen reactivity

We used a previously published variant of *C. hotsonii* CDH with a moderately (three times) increased H₂O₂ production rate (N700S) [28] as a template for semirational engineering. Further site-saturation mutagenesis was performed on residue N748 since studies on other FAD-dependent oxidases and monooxygenases had shown that this position on top of the isoalloxazine C4a position, which is adjacent to the reactive N5, influences the oxygen reactivity of flavoenzymes [29]. The proposed reaction mechanism for the reduction of O₂ proceeds via an initial electron transfer from the flavin hydroquinone to O₂ forming a superoxide anion (O₂^{•−}) followed by a spin inversion of the resulting caged radical pair. After spin inversion H₂O₂ is formed after a second electron transfer from the flavin semiquinone to the oxygen intermediate, which can proceed via the formation of either a transient C4a-hydroperoxy-flavin and subsequent decay to H₂O₂ or an outer sphere electron transfer [30,31]. The closest amino acid in CDH to the isoalloxazine C4a position is N748, which is also a neighbor of the catalytic H701 and therefore a hotspot for mutagenesis by influencing either the access of O₂ to the FAD or the electron transfer steps (Fig. 1). A phylogenetic analysis of 56 *cdh* sequences showed that N748 is highly conserved in CDHs and only one sequence from a hitherto

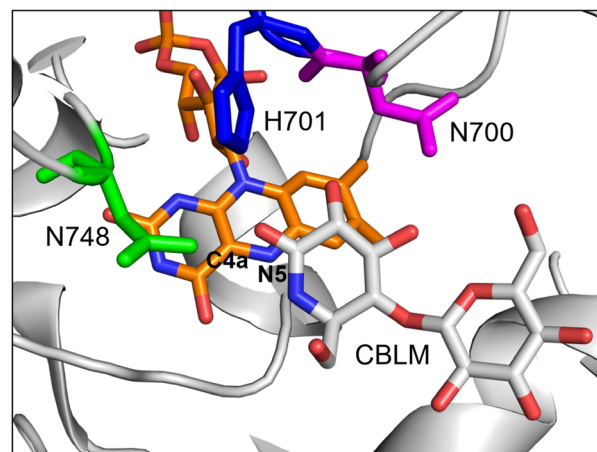


Fig. 1. The active site of *ChCDH* in complex with the inhibitor cellobionolactam (CBLM, pdb: 4QI5). Shown is the FAD-cofactor (orange) with the indicated C4a and N5 atoms and the catalytic base H701 (blue). The positions N700 (magenta) and N748 (green) of the wild-type *ChCDH* were replaced in this study by serine and glycine, respectively.

Table 1. Properties and catalytic activities of wild-type and recombinant enzymes.

Enzyme/ Variant	CYT domain	DH domain	Length (aa)	Mutations	Spec. activity, 2,6-dichloroindophenol (U·mg ⁻¹)	Spec. act. O ₂ (U·mg ⁻¹)	
						Cellobiose	Lactose
<i>Ch</i> CDH	yes	yes	806	none	0.82	0.015 ± 0.001	0.017 ± 0.001
CDH _{oxy+}	yes	yes	806	N700S/N748G	0.75	0.401 ± 0.019	0.368 ± 0.055
<i>Ch</i> DH	no	yes	576	none	1.42	0.016 ± 0.002	0.019 ± 0.002
DH _{oxy+}	no	yes	576	N700S/N748G	1.37	0.580 ± 0.019	0.396 ± 0.043

uncharacterized CDH contained a serine at the same position [32].

A site-saturation library of N748 was transformed in *Pichia pastoris* X-33 cells and was subjected to a high-throughput screening using the peroxidase-coupled ABTS (2,2'-azino-bis(3-ethylbenzothiazoline-6-sulphonic acid)) assay for detection of H₂O₂ production [28]. A second screening was based on the activity of CDH toward the artificial electron acceptor 2,6-dichloroindophenol to normalize the expression level of the enzyme variants [28].

In active *Ch*CDH variants, the substitution N748G showed the highest activity with O₂. The resulting double variant N748G/N700S was produced in both its

full-length form (CDH_{oxy+}) and in a truncated form (DH_{oxy+}), lacking the electron transferring cytochrome *b* domain [21] (Table 1). Steady-state kinetic experiments showed a 27- and 36-time higher specific activity of CDH_{oxy+} and DH_{oxy+}, respectively, over the wild-type enzymes (*Ch*CDH and *Ch*DH) when using the natural substrate cellobiose and O₂ as electron acceptor (Table 1). The turnover of the non-natural substrate lactose, which was used in later parts of this study for analytical reasons, was similarly enhanced. Interestingly, DH_{oxy+} showed a higher turnover than CDH_{oxy+}, which indicates that the cytochrome domain can kinetically impair the two-electron reduction of O₂ by removing one electron from FADH₂.

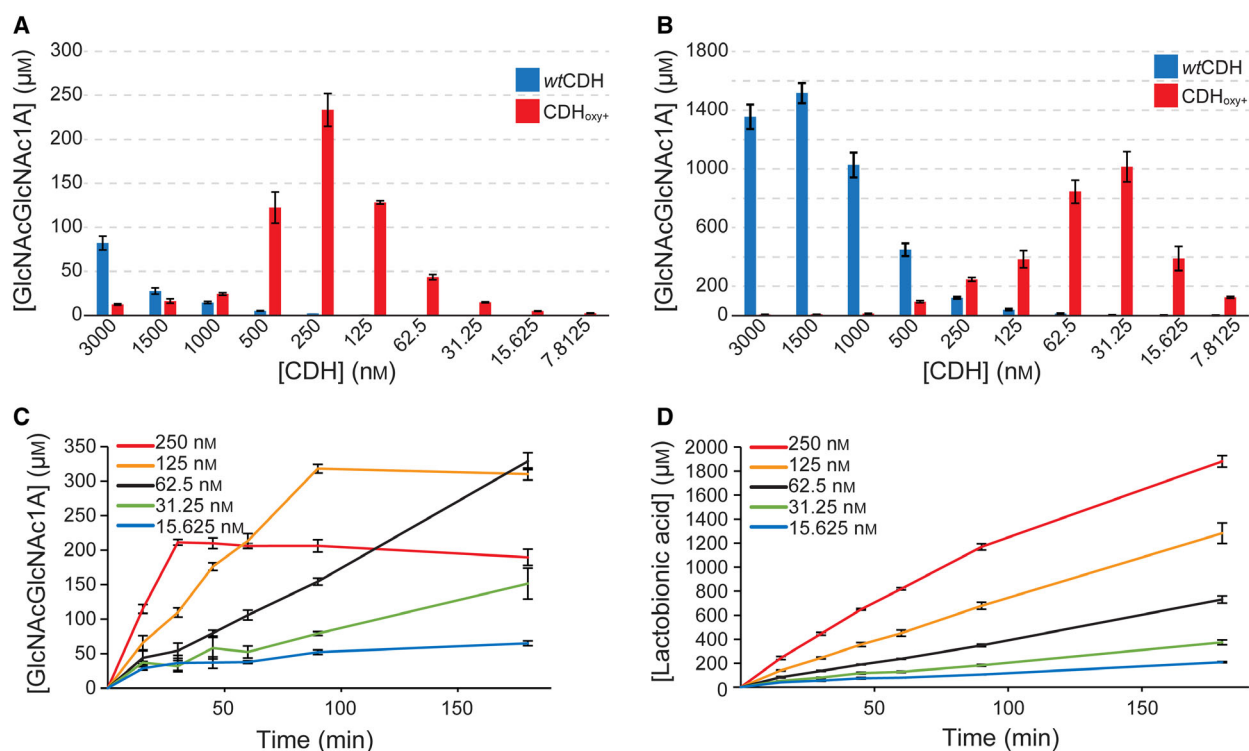


Fig. 2. Product formation by *Sm*LPMO10A. Chitobionic acid concentration after incubation of β -chitin with 1 μ M *Sm*LPMO10A, 15 mM lactose and 10 different concentrations of *Ch*CDH (blue) or CDH_{oxy+} (red) after 1 h (A) or 24 h (B). Panel (C) shows the time-dependent formation of chitobionic acid by *Sm*LPMO10A and (D) lactobionic acid by CDH_{oxy+} in reactions containing 1 μ M LPMO and five different concentrations of CDH_{oxy+}. All error bars show \pm S.D. ($n = 3$).

Activation of bacterial and fungal LPMOs by ChCDH

We initially tested the ability of CDH_{oxy+} to activate the bacterial C1-oxidizing chitin-active LPMO10A from *Serratia marcescens* (Fig. 2), which releases C1-oxidized chito-oligosaccharides as a product of the chitin oxidation reaction. Using lactose as a CDH substrate allowed a clear distinction between oxidation products generated by the LPMO (chito-oligosaccharides) and those generated by CDH (lactobionic acid) since the latter does not oxidize chito-oligosaccharides [33].

CDH_{oxy+} was more effective in driving the LPMO reaction when compared to the wild-type ChCDH. For example, after 1 h, we observed a 2.8-time higher LPMO product formation at a 12-time lower CDH_{oxy+} concentration (Fig. 2A; compare bars for 3000 nM ChCDH vs. 250 nM CDH_{oxy+}), which translates into CDH_{oxy+} being ~ 35 times more efficient in driving the LPMO reaction. Comparison with product concentrations obtained after 24 h showed a ~ 30 times higher efficiency (Fig. 2B; 1500 nM ChCDH vs. 31.25 nM

CDH_{oxy+}) but suggests considerable enzyme inactivation in reactions with higher CDH_{oxy+} concentrations. The nonlinear increase in the amount of reaction products from the 1- to 24-h experiments and the lower optimal CDH : LPMO ratios found in the 24-h experiment point toward a fast inactivation of one or both biocatalysts. We, therefore, analyzed the time-dependent formation of oxidation products from both CDH (lactobionic acid) and LPMO (oxidized chito-oligosaccharides). Data presented in Fig. 2C show that a high concentration of CDH_{oxy+} caused fast inactivation of the LPMO, while CDH activity was less affected (Fig. 2D). At low CDH_{oxy+} : LPMO ratios the LPMO activity was maintained throughout the reaction. This suggests LPMO inactivation when the rate of H₂O₂ production exceeded LPMO's capacity to convert its reactive cosubstrate in a productive manner, leading to H₂O₂-induced auto-oxidation reactions [15].

In all conversion experiments, the initial LPMO activity was linearly dependent on the H₂O₂ formation rate by CDH (Fig. 3). Quantitative analyses of both soluble and insoluble oxidized sites indicated that LPMO

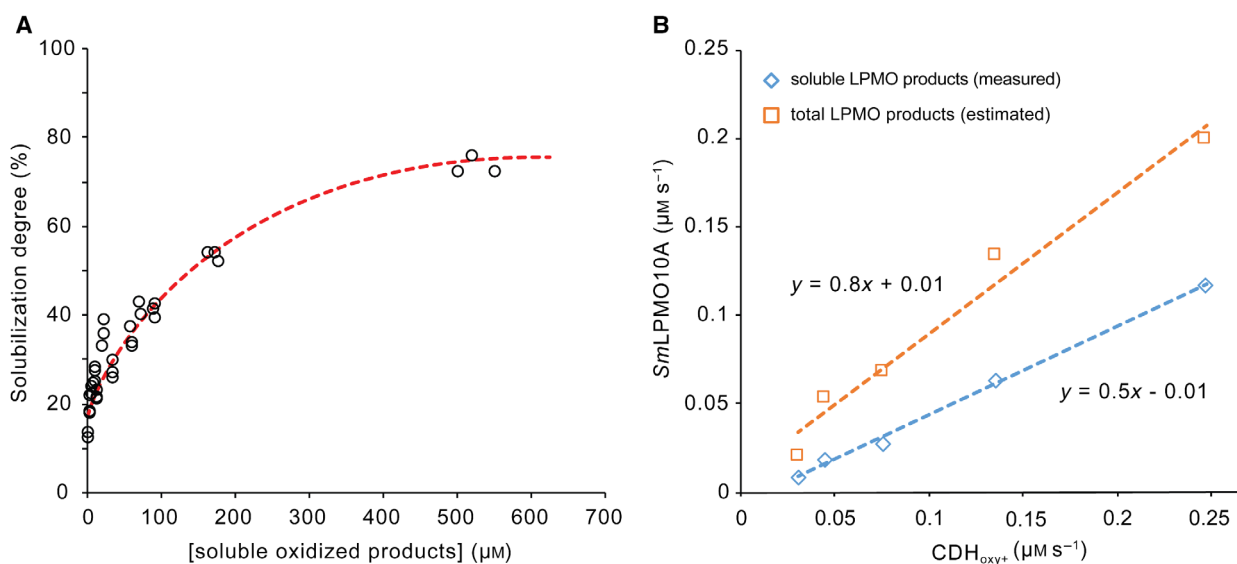


Fig. 3. Oxidized sites generated during chitin degradation by SmLPMO10A. Panel (A) shows a time-independent plot of the degree of solubilization of oxidized products (i.e., the percentage of products obtained in the soluble fraction compared to the total number of oxidized sites) as a function of the quantity of detected solubilized oxidized products. The total number of oxidized sites was determined in reactions containing 10 g·L⁻¹ β-chitin and 1 μM SmLPMO10A with varying concentrations of CDH_{oxy+} (31.25 or 125 nM) and 15 mM lactose. Samples were taken at different stages of the reaction (15–180 min). The samples were diluted twice and heat-inactivated (100 °C, 15 min). Half of the reaction was filtrated and 1 μM SmGH20 chitinase was added for quantitation of solubilized products (i.e., the standard procedure for quantitation of solubilized oxidized sites). To the other half of the reaction, a cocktail of chitinases (containing 2 μM SmChi18A, 2 μM SmChi18C and 1 μM SmGH20) was added followed by incubation for 20 h at 37 °C until the chitin was fully degraded. The resulting chitobionic acid concentration represents the total amount of oxidized sites. Rates derived from the initial phases of the progress curves in Fig. 2C,D only included time points where the solubilization was < 200 μM which means that the total number of oxidized sites is underestimated by ~ 50%. Panel (B) shows the LPMO activity without and with correction for this underestimation. The corrected curve shows that 1 molecule of lactose converted by CDH_{oxy+} leads to approximately 0.8 molecules of chitobionic acid being produced by SmLPMO10A.

catalyzed approximately 0.8 reactions per CDH-oxidized lactose molecule. The substoichiometric number in this experiment reflects CDH's dual role as a source of the cosubstrate and as an electron donor for LPMO.

When using the fungal *NcLPMO9C* in combination with *ChCDH* or CDH_{oxy+} , product chromatograms were dominated by double (C1/C4) oxidized products (Fig. 4) since CDH oxidizes the reducing end of the C4-oxidized products formed by the LPMO. The complex product spectrum of this reaction and the lack of suitable standards did not allow for a thorough analysis of the reaction kinetics. However, when comparing overall product peaks it becomes obvious that compared to reactions with *ChCDH* an ~ 24 time lower concentration of CDH_{oxy+} generated a similar product concentration (compare Fig. 4B vs. C). Note that in the reaction with high concentrations of CDH_{oxy+} (1.5 μM ; Fig. 4B) *NcLPMO9C* became rapidly inactivated, which corroborates the findings with *SmLPMO10A*.

Electron transfer rates of *ChCDH* and CDH_{oxy+}

We conducted rapid mixing experiments to probe CDH's internal electron transfer from the reduced $FADH_2$ to heme *b*. To this end, we mixed *ChCDH*

and CDH_{oxy+} with an excess of cellobiose and monitored both the reduction of the FAD (449 nm) and the heme *b* (563 nm) cofactors. For both CDH_{oxy+} and *ChCDH* the intramolecular electron transfer rates were similar at cellobiose concentrations higher than 1 mM ($0.35\text{--}0.48\text{ s}^{-1}$) (Fig. 5A). The lower electron transfer rates for CDH_{oxy+} at low cellobiose concentrations indicate competition for electrons between O_2 and the cytochrome domain at the DH domain (Fig. 5B).

The second, intermolecular electron transfer step from the reduced heme *b* to LPMO was probed by reacting prerduced CDH_{oxy+} with oxidized LPMO (Fig. 5C–E). Prerduction of CDH with cellobiose was performed under atmospheric conditions with or without catalase to investigate the effect of the by-product H_2O_2 on the observed rate. The presence of H_2O_2 had no effect on the LPMO reduction rate and in both cases, the apparent bimolecular rate constant for the CDH_{oxy+} /LPMO interaction was $1.27 \times 10^6\text{ M}^{-1}\cdot\text{s}^{-1}$, which is similar to the reported value for *ChCDH*/LPMO ($0.63 \times 10^6\text{ M}^{-1}\cdot\text{s}^{-1}$; [33]).

These experiments show that both *ChCDH* and CDH_{oxy+} have similar electron transferring capabilities under the tested conditions. We, therefore, conclude

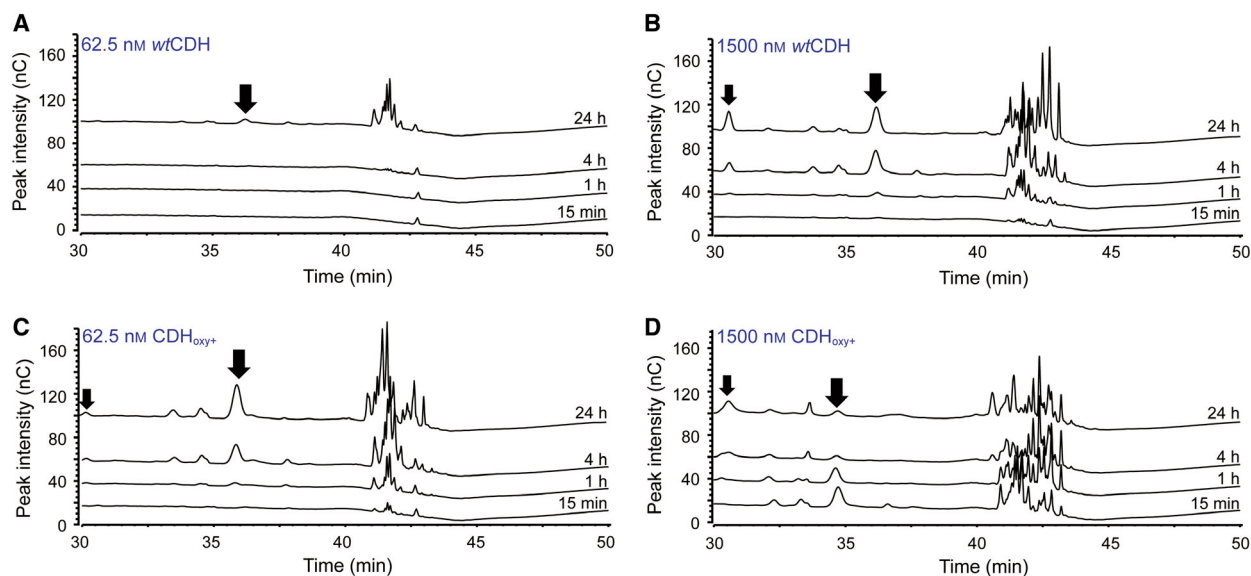


Fig. 4. Product formation by *NcLPMO9C*. HPAEC-PAD chromatograms show C4-oxidized products generated in reactions containing 1 μM *NcLPMO9C* in the presence of 62.5 nM (A) or 1500 nM *ChCDH* (B) and 62.5 nM (C) or 1500 nM CDH_{oxy+} (D). All reactions contained 5 $\text{g}\cdot\text{L}^{-1}$ PASC and 15 mM lactose and were incubated in 50 mM potassium phosphate buffer, pH 6.0, for up to 24 h in an Eppendorf thermomixer (Hamburg, Germany) set to 30 $^{\circ}\text{C}$ and 800 r.p.m. Samples were heat-inactivated (15 min, 100 $^{\circ}\text{C}$) and filtered (0.22 μm) prior to analysis. The bigger black arrows indicate the Glc4GemGlc C4-oxidized product, whereas the smaller black arrows, seen in panel (B–D), show Glc₂Glc1A peaks that are formed as a result of CDH oxidation of the native cellotriose that is formed by the LPMO upon cleavage of shorter cello-oligosaccharides. Peak annotations are based on earlier studies [41,42]. Note that the elution times vary slightly between different runs. Double (C1/C4) oxidized products (peaks eluting after ~ 40 min) dominate since CDH oxidizes the reducing end of the C4-oxidized products formed by the LPMO. Note that C4-oxidized products are unstable, which explains why some peaks become smaller over time in panel (D).

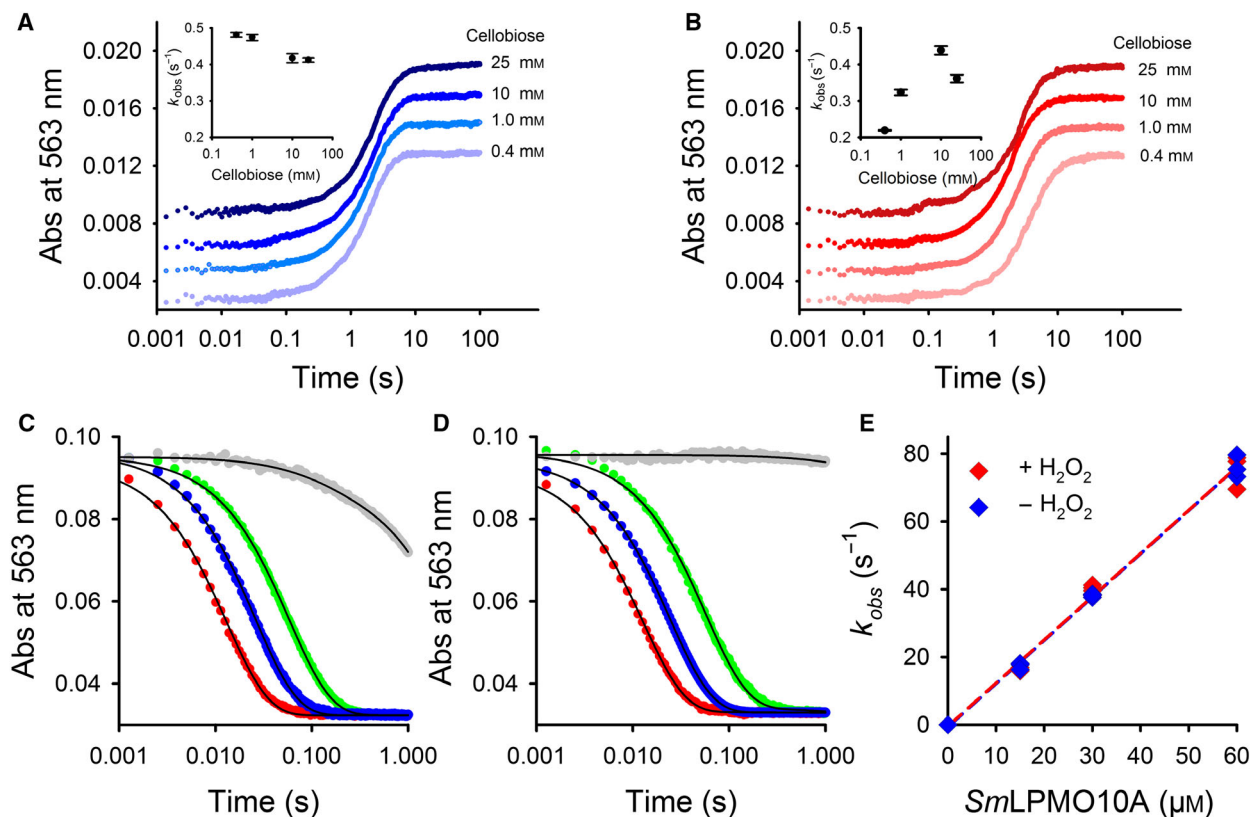


Fig. 5. Electron transfer between redox centers. Intramolecular electron transfer in *ChCDH* (A) and CDH_{ox^+} (B) from FAD, in the DH domain, to heme *b*, in the cytochrome domain, at the indicated cellobiose concentrations. Heme *b* reduction was followed at 563 nm (α -band). The concentration of CDH after mixing was 1.5 μM . Prior to all measurements, substrate and enzyme solutions were carefully degassed by applying alternating cycles of vacuum and nitrogen pressure to avoid interference with atmospheric oxygen. All measurements were carried out at 30 °C in 50 mM sodium phosphate buffer, pH 6.0. The insets show the cellobiose concentration-dependent electron transfer rates. Panels (C) and (D) show raw traces for heme *b* reoxidation by *SmLPMO10A* in the absence (catalase added, C) or presence (no catalase added, D) of H_2O_2 using 0 μM (gray), 15 μM (green), 30 μM (blue) or 60 μM (red) LPMO. (E) Electron transfer from reduced heme *b* to LPMO in the presence (red) or absence (blue) of approximately 250 μM H_2O_2 formed by CDH during prereduction. All traces are the average of triplicate measurements. Error bars show \pm S.D. ($n = 3$).

that the increased ability of CDH_{ox^+} to support LPMO reactions is not caused by changes in the ability to reduce the LPMO but to increase production of H_2O_2 .

Activation of LPMO by *ChDH* and DH_{ox^+}

To gain further insight into the CDH-LPMO interplay, we replaced the full-length enzymes in conversion experiments with DH_{ox^+} and *ChDH* at concentrations (31.25 and 750 nM, respectively) expected to produce the same amount of H_2O_2 . Unexpectedly, in the absence of an additional reductant like ascorbic acid (AscA), both dehydrogenase domains were capable of driving the LPMO reaction to some extent, despite the lack of an electron transferring cytochrome domain (Fig. 6). The DH domain of *ChCDH* was previously shown to be incapable of direct electron transfer to

LPMO [21], but activation of LPMO by some flavoenzymes without cytochrome domains under steady-state conditions has been reported [34]. Considering that all the investigated flavoenzymes bind FAD noncovalently and that in our experiments *ChDH* (at 750 nM) was much more effective than DH_{ox^+} (at 31.25 nM) at initiating LPMO activity (Fig. 6A), we considered FAD itself as a potential redox mediator between LPMO and DH. Thus, as a control, we carried out reactions with added FAD and compared it with reactions supplemented with the commonly used reductant AscA. Adding 0.25 mM FAD or 0.1 mM AscA to reactions containing 750 nM *ChDH* led to a slight increase in the amount of formed LPMO reaction products (Fig. 6B). A doubling of LPMO activity was observed upon adding FAD to reactions containing 31.25 nM DH_{ox^+} , whereas in this case, the addition of 0.1 mM

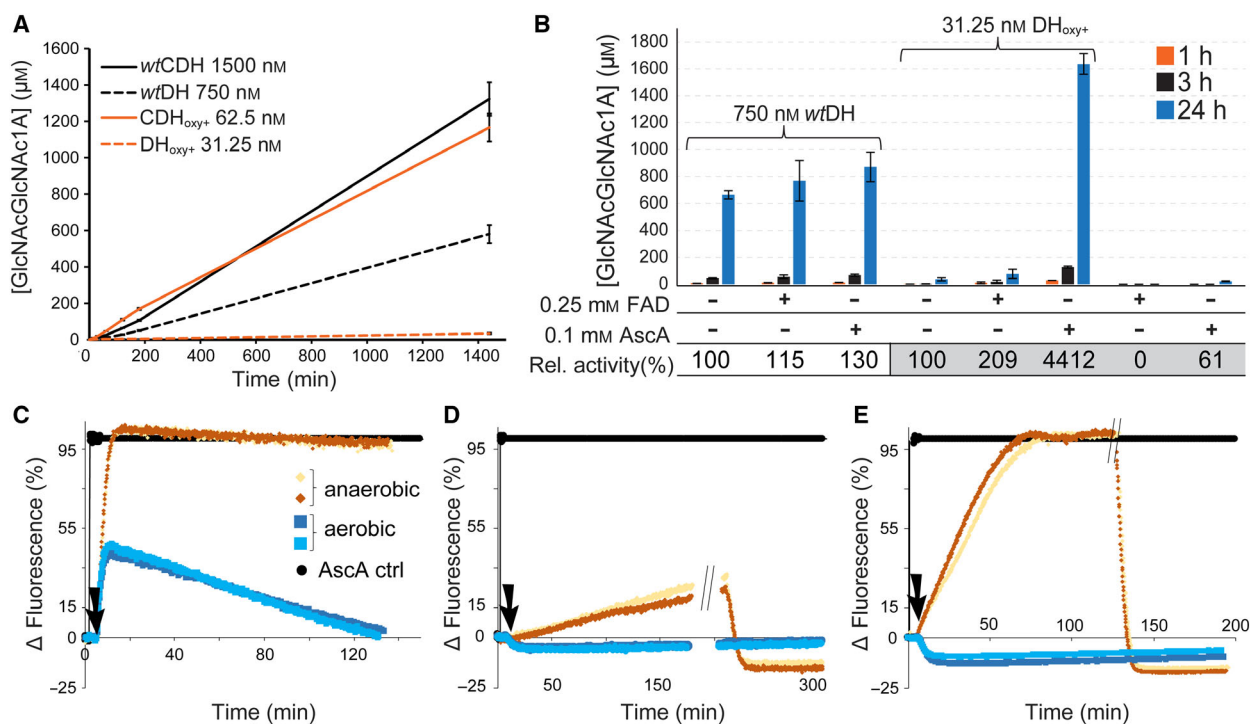


Fig. 6. LPMO activity driven by CDH without the cytochrome domain. (A) Time courses of chitobionic acid production by 1 μM *SmLPMO10A* in combination with CDH variants. (B) Quantitation of LPMO products generated in reactions containing 0.25 mM FAD or 0.1 mM ascorbic acid (AscA) in the presence or absence of 750 nM *ChDH* or 31.25 nM DH_{oxy+}. Relative activities show the enhancement upon addition of FAD or AscA (based on product levels after 24 h). The error bars show \pm S.D. ($n = 3$). Lower panels: Reduction of *SmLPMO10A* by different CDH variants under anaerobic or aerobic conditions. All reactions contained 2 μM *SmLPMO10A* and 0.25 μM *ChDH* (C); 0.25 μM *ChDH* (D); or 31.25 nM DH_{oxy+} (E). Reactions were initiated by addition of lactose (1 mM final concentration, black arrow) and were performed in duplicate (both traces are displayed). The variation in fluorescence is relative to the maximum increase in fluorescence measured for a control reaction (black line) in which lactose was replaced by 10 μM AscA, which represents a 100% reduction of *SmLPMO10A*. The "//" labels in panel (D) and (E) indicate when the reactions were no longer under anaerobic conditions.

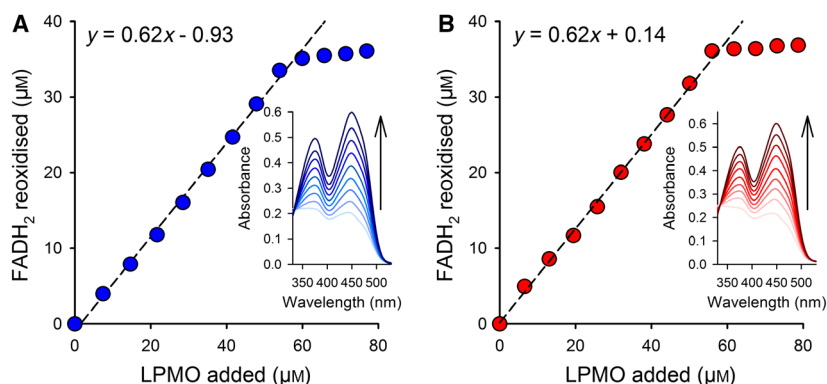


Fig. 7. Stoichiometry of LPMO reduction with FADH₂. Titration of FADH₂ with *NcLPMO9C* (A) or *SmLPMO10A* (B). Oxidized FAD (60 μM) was approximately 70% reduced with sodium dithionite. The FADH₂ was reoxidized with LPMO by adding aliquots of 3 μL (*NcLPMO9C*; 515 μM) or 1.5 μL (*SmLPMO10A*; 906 μM) to the cuvette. Absorption spectra were recorded with an Agilent 8453 UV/VIS-Spectrometer featuring a diode array detector. Blank reactions (buffer titrated to FADH₂ or LPMO) were subtracted. The concentration of FAD and LPMOs was determined based on their molar absorption coefficients (FAD $\epsilon_{450} = 11.3 \text{ mM}^{-1}\cdot\text{cm}^{-1}$; *NcLPMO9C* $\epsilon_{280} = 46.91 \text{ mM}^{-1}\cdot\text{cm}^{-1}$; *SmLPMO10A* $\epsilon_{280} = 35.20 \text{ mM}^{-1}\cdot\text{cm}^{-1}$). All reactions were carried out at 23 °C in an anaerobic glove box (Whitley DG250, Don Whitley Scientific) flushed with a nitrogen/hydrogen mixture. The data show that, for both LPMOs, about two molecules of enzyme were required to reoxidize 1 molecule of FADH₂.

AscA led to a much higher, 55-fold, increase in the LPMO product concentration after 24 h. These observations show that FAD can act as a redox mediator between the DH domain and the LPMO. The strong effect of AscA on the reactions with $\text{DH}_{\text{oxy}+}$ demonstrates that at low DH concentrations the concentration of dissociated FAD, and, thus, reduction of the LPMO becomes rate limiting. In this case, the addition of another reductant (AscA) alleviates the limitation and enables the LPMO to convert the available H_2O_2 . Titrations of FADH_2 with oxidized *Sm*LPMO10A and *Nc*LPMO9C (Fig. 7) confirmed that FADH_2 indeed reduces both enzymes with the expected 1 : 2 stoichiometry (1 electron per LPMO active site copper), underpinning the potential of FADH_2/FAD redox cycling between DH and LPMO. Whether dissociated FADH_2 is of relevance as a natural redox mediator system is debatable, since the DH concentration in the experiments was higher than those usually observed *in vivo*.

We also considered that superoxide, generated via a one-electron reduction of O_2 at the cytochrome domain, could act as a potential reductant for LPMO. Such a reduction was previously shown to occur at high superoxide concentrations, albeit with low efficiency [15]. Using a fluorescence-based assay [35] we observed that under anaerobic conditions *Ch*CDH reduced LPMO completely, while under aerobic conditions only 45% of the LPMO was reduced due to simultaneous reoxidation of CDH by O_2 (Fig. 6C). The fact that both *Ch*CDH and $\text{DH}_{\text{oxy}+}$ reduced LPMO under anaerobic conditions (Fig. 6D,E) indicates that LPMO reduction by these truncated enzymes does not involve superoxide and is rather due to FADH_2/FAD redox cycling, as discussed above.

Conclusions

Taken together, these experiments support the importance of H_2O_2 -driven LPMO catalysis. While *Ch*CDH and $\text{CDH}_{\text{oxy}+}$ transfer electrons to the LPMO with similar efficiencies, they produce different amounts of H_2O_2 , which translates into different LPMO activities. In accordance with the correlation between H_2O_2 production by the CDH and LPMO activity, it has been noted earlier that the rate of *Ch*CDH-driven LPMO activity is similar to the rate of H_2O_2 production by *Ch*CDH in reactions with O_2 as the only electron acceptor [33]. It has been suggested that H_2O_2 -driven LPMO activity implies that, when once reduced, an LPMO could carry out multiple oxidative cleavages [15]. The apparent stoichiometry of the reactions that may be derived from the data displayed in Fig. 3 is

compatible with these previous observations: our data show that approximately 8 out of 10 oxidized substrate molecules of $\text{CDH}_{\text{oxy}+}$ are used to generate H_2O_2 , which is stoichiometrically used for polysaccharide cleavage. The remaining two substrate molecules can generate four reduction equivalents for the reduction of LPMO, meaning that at least two H_2O_2 molecules are consumed per LPMO reduction. Studies with externally added reductant and H_2O_2 have shown that under certain conditions a reduced LPMO may catalyze 15–18 reactions [15,36].

The cytochrome domain allows for specific intermolecular electron transfer from CDH to LPMO, but LPMO reduction can also be accomplished by a small molecule reductant like AscA or, interestingly, also by FADH_2 when the flavodehydrogenase is applied at high concentrations. The exact mechanism of LPMO activation is currently disputed [15,18]. In light of this debate, it is worth noting the AscA experiments depicted in Fig. 6B: the amount of oxidized products generated after 24 h in a reaction containing 0.1 mM AscA and 31.25 nM $\text{DH}_{\text{oxy}+}$ was 72 times higher when compared to a reaction containing only 0.1 mM AscA. This difference supports the hypothesis that under commonly employed reaction conditions in LPMO experiments the production of H_2O_2 is rate limiting.

Aside from providing novel insight into H_2O_2 -driven LPMO catalysis and providing a newly engineered enzyme, $\text{CDH}_{\text{oxy}+}$, with potential applications in industrial biomass processing, the present study sheds light on a rarely investigated biological role of CDH. The very low O_2 turnover of CDHs might provide a slow but steady H_2O_2 supply for LPMOs in a physiological setting, thereby avoiding oxidative damage of LPMO.

Materials and methods

Generation of *Ch*CDH and $\text{CDH}_{\text{oxy}+}$

The codon-optimized expression plasmid pPIC-MtSopt encoding the full-length wild-type CDH from the thermophilic fungus *C. hotsonii* (syn. *M. thermophilum*; *Ch*CDH) under the control of the methanol-inducible AOX promoter was used as a parental plasmid for the generation of $\text{CDH}_{\text{oxy}+}$. In a previous study, we already used this plasmid as a template for a semirational approach resulting in variant N700S with a moderately improved H_2O_2 production rate [28]. In the present study, the plasmid pPIC-MtCDH N700S encoding the above-mentioned variant was used as the starting point for an additional round of protein engineering by site-saturation mutagenesis. A *cdh* library containing all possible codons at the targeted

position N748 was prepared using the forward primer: TACCACTNNSCCAATTCTTACATTGTCG and the reverse primer: AAGTTGGSNAGTGGTAGGAA-CACC. A library of 368 clones was screened by a differential screening using the peroxidase-coupled ABTS assay for detection of H₂O₂ production and the 2,6-dichloroindophenol assay to normalize the expression level of the enzyme variants [28]. In this screening, five variants showed an increased H₂O₂ production compared to the parental enzyme N700S. The sequencing results showed that all of them carried the additional mutation N748G. With respect to its increased oxygen reactivity, the identified *Ch*CDH variant N700S/N748G was named CDH_{oxy+}.

Generation of *Ch*DH and DH_{oxy+}

To obtain CDH and its oxygen-converting variant without the electron-transferring cytochrome domain, two truncated sequences (expression plasmids pPIC-wtDH and pPIC-DH_{oxy+}) were synthesized by a commercial provider (ATG: biosynthetics, Merzhausen, Germany). In both plasmids, the sequence encoding for the native signal sequence (nucleotides 1–63) was directly followed by the dehydrogenase domain encoding sequence [nucleotides 750–2481 (F230–L806)]. The 687 nucleotides encoding for the cytochrome domain and the interdomain linker (N1–S229) were omitted in pPIC-wtDH. The expression plasmid pPIC-DH_{oxy+} additionally carried the two mutations N700S and N748G.

Heterologous production and purification

All four enzymes were recombinantly produced in *P. pastoris* X-33 cells and purified as previously reported [37]. Table 1 shows the activities of the CDH and DH variants which were measured with 2,6-dichloroindophenol as a chromogenic electron acceptor and 30 mM lactose as a substrate in 50 mM potassium phosphate buffer, pH 6.0. Data are expressed as mean values ± SD from three measurements. The calculated molar absorption coefficients at 280 nm given in Table 1 were used to calculate the protein concentrations and the specific activities.

The LPMO 10A from *S. marcescens* (*Sm*LPMO10A, also known as CBP21) was recombinantly produced in *Escherichia coli* and purified by chitin affinity chromatography as previously described [38]. A threefold molar surplus of Cu(II) SO₄ was added to the pure protein to ensure that each LPMO molecule has a copper cofactor. Excess copper was removed by applying the LPMO-copper solution on a PD Midi-Trap G-25 column (GE Healthcare, Vienna, Austria) equilibrated with 50 mM potassium phosphate buffer, pH 6.0. The protein concentration was determined by measuring A280 using the calculated molar absorption coefficient of 35.20 mm⁻¹·cm⁻¹.

The LPMO 9C from *Neurospora crassa* (*Nc*LPMO9C, previously termed PMO-02916) was recombinantly produced in *P. pastoris* in a bioreactor and purified by a two-step

chromatographic procedure as previously described [39]. The purified enzyme solution was repeatedly diafiltered against 50 mM potassium phosphate buffer, pH 6.0. The protein concentration was determined by measuring A280 using the calculated molar absorption coefficient of 46.91 mm⁻¹·cm⁻¹.

Oxygen reactivity of CDH variants

The oxygen turnover of *Ch*CDH and CDH variants was measured by incubating either 1.5 μM of the CDH and DH with low oxygen turnover (*Ch*CDH and *Ch*DH) or 30 nM of the CDH and DH variants with high oxygen turnover (CDH_{oxy+} and DH_{oxy+}) with 5 mM cellobiose or lactose. Reactions had a total volume of 500 μL and were incubated at 40 °C in 50 mM sodium phosphate buffer, pH 6.0, at a constant agitation of 800 r.p.m. Samples were withdrawn regularly, incubated at 95 °C for 10 min to stop the reaction and measured by HPLC for aldonic acid formation.

Standard LPMO/CDH reactions

Standard reactions were set up with 1 μM *Sm*LPMO10A and 10 g·L⁻¹ β-chitin, 15 mM lactose and the different CDH variants (i.e., *Ch*CDH, CDH_{oxy+}, *Ch*DH, or DH_{oxy+}) with concentrations varying from 7.8 to 3000 nM. When using the truncated DH variants, lower concentrations were used as these variants produce more H₂O₂ compared to the full-length enzymes. All reactions were carried out in 50 mM potassium phosphate buffer, pH 6.0, in a Thermomixer set to 30 °C and 800 r.p.m. At regular intervals, samples were taken from the reactions, and the LPMO activity was stopped by directly separating the soluble fractions from the insoluble chitin particles by filtration using a 96-well filter plate (Millipore, Burlington, MA, USA) operated with a vacuum manifold. For samples where both aldonic acids from the LPMO and CDH (i.e., chitobionic acid and lactobionic acid) were subjected to quantitative analysis, the enzyme reaction was first stopped by 15 min heat inactivation at 100 °C followed by filtration (0.22 μm). *Sm*LPMO10A-generated chito-oligosaccharides were further degraded by incubation with 1 μM *Sm*GH20 chitinase as previously described [40] to produce *N*-acetyl-glucosamine and chitobionic acid, where the latter product represents the sum of all solubilized oxidized sites. To determine the total oxidized products, the LPMO reactions were stopped by heat inactivation (100 °C, 15 min) followed by 20 h of incubation with 2 μM of the *S. marcescens* exo-chitinase A (*Sm*Chi18A) and 2 μM endo-chitinase (*Sm*Chi18C) as well as 1 μM *Sm*GH20 chitinase.

Quantitation of aldonic acids

Aldonic acids generated by CDH were quantified following two previously published HPLC methods [41,42]. Quantitation of GlcNAcGlcNAc1A (i.e., chitobionic acid) from reactions containing *Sm*LPMO10A was accomplished using

an RSLC system (Dionex, Sunnyvale, CA, USA) equipped with a 100×7.8 -mm Rezex RFQ-Fast Acid H+ (8 %) (Phenomenex, Torrance, CA, USA) column operated at 85 °C. Samples of 8 μL were injected into the column and solutes were eluted isocratically using 5 mM sulfuric acid as mobile phase with a flow rate of $1 \text{ mL}\cdot\text{min}^{-1}$. The elution of products was monitored and recorded at 194 nm.

In-house made chitobionic acid solutions with known concentrations were used to generate a standard curve of oxidized products. Briefly, $(\text{GlcNAc})_2$ was dissolved to a final concentration of 5.0 mM in 50 mM Tris/HCl pH 8.0 and incubated overnight with $0.12 \text{ mg}\cdot\text{mL}^{-1}$ *Fusarium graminearum* chito-oligosaccharide oxidase [43] at 20 °C as previously described [40] to generate chitobionic acid (i.e., GlcNAcGlcNAc1A).

Rapid kinetic studies of cellobiose dehydrogenase

Rapid kinetic experiments were performed with an SX20 stopped-flow spectrophotometer (Applied Photophysics, Leatherhead, UK) using a photomultiplier tube (PMT) detector. All experiments were performed in 50 mM sodium phosphate buffer, pH 6.0, at 30 °C. Substrate and enzyme solutions were degassed prior to all measurements unless stated otherwise. The cellobiose-dependent reduction of the CDH cytochrome domain was measured in single mixing mode by following the absorbance at 563 nm (heme α -band). For the determination of the interdomain FAD-to-heme b electron transfer, CDH and cellobiose were used at final concentrations of 1.5 μM and 0.4–25 mM, respectively. Electron transfer from the reduced heme b to *Sm*LPMO10A was studied in sequential mixing mode. Initially, CDH (20 μM) was mixed with 5 mM of cellobiose in an aging loop until the full reduction of the heme b cofactor was observed (320 s). The reduced enzyme was rapidly mixed with *Sm*LPMO10A (15–60 μM) or buffer. These experiments were performed aerobically at a dissolved oxygen concentration of 250 μM . Approximately the same concentration of H_2O_2 was accumulated during prereduction of CDH with cellobiose in the aging loop. The same experiments were therefore performed in the presence of 500 $\text{U}\cdot\text{mL}^{-1}$ catalase from *Corynebacterium glutamicum* (Sigma Aldrich, St. Louis, MO, USA) in the aging loop to remove H_2O_2 before reacting the enzyme with LPMO. The required aging time in these experiments was 360 s. Observed rates (k_{obs}) were determined by fitting the initial slope of at least three experimental repeats to an exponential function using the PRO DATA SX software (Applied Photophysics).

Titration of *Sm*LPMO10A and *Nc*LPMO9C with FADH_2

All experiments were performed in 50 mM sodium phosphate buffer, pH 6.0, in an anaerobic glove box (Whitley

DG250; Don Whitley Scientific, Shipley, UK), which was continuously flushed with a nitrogen/hydrogen mixture (90/10). Residual oxygen was removed with a palladium catalyst and the generated water vapor was absorbed by silica gel. To probe the interaction of FADH_2 with LPMO, oxidized FAD (60 μM) was approximately 70% reduced with sodium dithionite to avoid an excess of reductant. FADH_2 was reoxidized with LPMO by adding aliquots of 3 μL Cu (II)-loaded *Nc*LPMO9C from a 515 μM stock solution or 1.5 μL Cu(II)-loaded *Sm*LPMO10A from a 906 μM stock solution to the cuvette. Spectra were recorded after mixing. Blank runs containing FADH_2 in buffer or LPMO in buffer were subtracted from these spectra. Electronic absorption spectra were recorded with an Agilent 8453 UV-visible spectrophotometer (Santa Clara, CA, USA) equipped with a photodiode array detector. All reagents and enzyme solutions used in the glove box were extensively degassed by applying alternate cycles of vacuum and nitrogen pressure. All experiments were carried out in quartz cuvettes (200 μL total volume) at a constant temperature of 25 °C.

Monitoring the redox state of *Sm*LPMO10A by fluorimetry

All reactions were carried out in 50 mM potassium phosphate buffer, pH 6.0 at 25 °C, prepared under aerobic or anaerobic conditions, and contained 2 μM *Sm*LPMO10A mixed with either *Ch*CDH (0.25 μM) or *Ch*DH (0.25 μM) or $\text{DH}_{\text{oxy}+}$ (31.25 nM). Enzyme mixtures were transferred to a sealable fluorescence quartz cuvette equipped with screw cap and septum (Hellma, Müllheim, Germany), which was inserted into a Cary Eclipse Fluorescence spectrophotometer (Agilent Technologies, Santa Clara, CA, USA). Excitation and emission wavelengths were set to 280 and 340 nm, respectively, and the PMT detector voltage set to 550 V, as previously described [35]. Reactions were initiated by addition of lactose (1 mM final concentration) using a Hamilton syringe. In a control reaction, carried out in anaerobic conditions, the lactose/CDH system was replaced by AscA (10 μM final concentration) to reduce the LPMO, providing a reference fluorescence signal corresponding to 100% reduction of *Sm*LPMO10A. All fluorescence signals were expressed as the variation in fluorescence relative to the maximum increase observed in this control reaction.

Acknowledgements

This work was supported by the Austrian Science Fund FWF through grants J4154 (DK), W1224, and I2385-N28 (RL), and the Research Council of Norway, through grants 240967, 243663, and 262853 (VGHE).

Conflict of interest

The authors declare no conflict of interest.

Author contributions

DK planned, performed, and interpreted oxygen conversion, rapid kinetic and anaerobic titration experiments, and wrote the original draft of the manuscript; ZF planned, performed, and interpreted conversion and electron transfer experiments and contributed to the original draft; BB planned, performed, and interpreted oxidation studies and fluorescence experiments; SG supported conversion and oxidation studies; MP and CS generated, produced, and purified the CDH variants and characterized them; VGHE and RL equally planned the study, acquired funding and administrated the project, supported the evaluation and interpretation of experiments, and wrote the final version of the manuscript.

References

- Vaaje-Kolstad G, Westereng B, Horn SJ, Liu Z, Zhai H, Sørlie M, Eijsink VGH (2010) An oxidative enzyme boosting the enzymatic conversion of recalcitrant polysaccharides. *Science* **330**, 219–222.
- Quinlan RJ, Sweeney MD, Lo Leggio L, Otten H, Poulsen J-CN, Johansen KS, Krogh KBRM, Jørgensen CI, Tovborg M, Anthonsen A *et al.* (2011) Insights into the oxidative degradation of cellulose by a copper metalloenzyme that exploits biomass components. *Proc Natl Acad Sci USA* **108**, 15079–15084.
- Sabbadin F, Hemsworth GR, Ciano L, Henrissat B, Dupree P, Tryfona T, Marques RDS, Sweeney ST, Besser K, Elias L *et al.* (2018) An ancient family of lytic polysaccharide monoxygenases with roles in arthropod development and biomass digestion. *Nat Commun* **9**, 756.
- Couturier M, Ladevèze S, Sulzenbacher G, Ciano L, Fanuel M, Moreau C, Villares A, Cathala B, Chaspoul F, Frandsen KE *et al.* (2018) Lytic xylan oxidases from wood-decay fungi unlock biomass degradation. *Nat Chem Biol* **14**, 306–310.
- Vu VV, Beeson WT, Span EA, Farquhar ER & Marletta MA (2014) A family of starch-active polysaccharide monoxygenases. *Proc Natl Acad Sci USA* **111**, 13822–13827.
- Langston JA, Shaghasi T, Abbate E, Xu F, Vlasenko E & Sweeney MD (2011) Oxidoreductive cellulose depolymerization by the enzymes cellobiose dehydrogenase and glycoside hydrolase 61. *Appl Environ Microbiol* **77**, 7007–7015.
- Eibinger M, Ganner T, Bubner P, Rošker S, Kracher D, Haltrich D, Ludwig R, Plank H & Nidetzky B (2014) Cellulose surface degradation by a lytic polysaccharide monoxygenase and its effect on cellulase hydrolytic efficiency. *J Biol Chem* **289**, 35929–35938.
- Song B, Li B, Wang X, Shen W, Park S, Collings C, Feng A, Smith SJ, Walton JD & Ding SY (2018) Real-time imaging reveals that lytic polysaccharide monoxygenase promotes cellulase activity by increasing cellulose accessibility. *Biotechnol Biofuels* **11**, 41.
- Beeson WT, Phillips CM, Cate JHD & Marletta MA (2012) Oxidative cleavage of cellulose by fungal copper-dependent polysaccharide monoxygenases. *J Am Chem Soc* **134**, 890–892.
- Walton PH & Davies GJ (2016) On the catalytic mechanisms of lytic polysaccharide monoxygenases. *Curr Opin Chem Biol* **31**, 195–207.
- Phillips CM, Beeson WT, Cate JH & Marletta MA (2011) Cellobiose dehydrogenase and a copper-dependent polysaccharide monoxygenase potentiate cellulose degradation by *Neurospora crassa*. *ACS Chem Biol* **6**, 1399–1406.
- Kjaergaard CH, Qayyum MF, Wong SD, Xu F, Hemsworth GR, Walton DJ, Young NA, Davies GJ, Walton PH, Johansen KS *et al.* (2014) Spectroscopic and computational insight into the activation of O₂ by the mononuclear Cu center in polysaccharide monoxygenases. *Proc Natl Acad Sci USA* **111**, 8797–8802.
- O'Dell WB, Agarwal PK & Meilleur F (2017) Oxygen activation at the active site of a fungal lytic polysaccharide monoxygenase. *Angew Chemie Int Ed Engl* **56**, 767–770.
- Kittl R, Kracher D, Burgstaller D, Haltrich D & Ludwig R (2012) Production of four *Neurospora crassa* lytic polysaccharide monoxygenases in *Pichia pastoris* monitored by a fluorimetric assay. *Biotechnol Biofuels* **5**, 79.
- Bissaro B, Røhr ÅK, Müller G, Chylenski P, Skaugen M, Forsberg Z, Horn SJ, Vaaje-Kolstad G & Eijsink VGH (2017) Oxidative cleavage of polysaccharides by monocopper enzymes depends on H₂O₂. *Nat Chem Biol* **13**, 1123–1128.
- Kuusk S, Bissaro B, Kuusk P, Forsberg Z, Eijsink VGH, Sørlie M & Valjamae P (2018) Kinetics of H₂O₂-driven degradation of chitin by a bacterial lytic polysaccharide monoxygenase. *J Biol Chem* **293**, 523–531.
- Kim S, Ståhlberg J, Sandgren M, Paton RS & Beckham GT (2014) Quantum mechanical calculations suggest that lytic polysaccharide monoxygenases use a copper-oxygen rebound mechanism. *Proc Natl Acad Sci USA* **111**, 149–154.
- Hangasky JA, Iavarone AT, Marletta MA, Karlin KD & Stubbe J (2018) Reactivity of O₂ versus H₂O₂ with polysaccharide monoxygenases. *Proc Natl Acad Sci USA* **115**, 4915–4920.
- Müller G, Chylenski P, Bissaro B, Eijsink VGH & Horn SJ (2018) The impact of hydrogen peroxide supply on LPMO activity and overall saccharification

- efficiency of a commercial cellulase cocktail. *Biotechnol Biofuels* **11**, 209.
- 20 Kracher D, Scheiblbrandner S, Felice AKG, Breslmayr E, Preims M, Ludwicka K, Haltrich D, Eijsink VGH & Ludwig R (2016) Extracellular electron transfer systems fuel cellulose oxidative degradation. *Science* **352**, 1098–1101.
- 21 Tan T-C, Kracher D, Gandini R, Sygmond C, Kittl R, Haltrich D, Hällberg BM, Ludwig R & Divne C (2015) Structural basis for cellobiose dehydrogenase action during oxidative cellulose degradation. *Nat Commun* **6**, 7542.
- 22 Wilson MT, Hogg N & Jones GD (1990) Reactions of reduced cellobiose oxidase with oxygen. Is cellobiose oxidase primarily an oxidase? *Biochem J* **270**, 265–267.
- 23 Bao WJ, Usha SN & Renganathan V (1993) Purification and characterization of cellobiose dehydrogenase, a novel extracellular hemoflavoenzyme from the white-rot fungus *Phanerochaete chrysosporium*. *Arch Biochem Biophys* **300**, 705–713.
- 24 Pricelius S, Ludwig R, Lant N, Haltrich D & Guebitz GM (2009) Substrate specificity of *Myriococcum thermophilum* cellobiose dehydrogenase on mono-, oligo-, and polysaccharides related to *in situ* production of H₂O₂. *Appl Microbiol Biotechnol* **85**, 75–83.
- 25 Bissaro B, Varnai A, Røhr ÅK & Eijsink VGH (2018) Oxidoreductases and reactive oxygen species in lignocellulose biomass conversion. *Microbiol Mol Biol Rev* **4**, 1–51.
- 26 Kracher D, Zahma K, Schulz C, Sygmond C, Gorton L & Ludwig R (2015) Inter-domain electron transfer in cellobiose dehydrogenase: Modulation by pH and divalent cations. *FEBS J* **282**, 3136–3148.
- 27 Breslmayr E, Hanžek M, Hanrahan A, Leitner C, Kittl R, Šantek B, Oostenbrink C & Ludwig R (2018) A fast and sensitive activity assay for lytic polysaccharide monoxygenase. *Biotechnol Biofuels* **11**, 1–13.
- 28 Sygmond C, Santner P, Krondorfer I, Peterbauer CK, Alcalde M, Nyanhongo GS, Guebitz GM & Ludwig R (2013) Semi-rational engineering of cellobiose dehydrogenase for improved hydrogen peroxide production. *Microb Cell Fact* **12**, 38.
- 29 Bruice TC (1984) Oxygen-flavin chemistry. *Isr J Chem* **21**, 54–61.
- 30 Romero E, Gómez Castellanos JR, Gadda G, Fraaije MW & Mattevi A (2018) Same substrate, many reactions: oxygen activation in flavoenzymes. *Chem Rev* **118**, 1742–1769.
- 31 Gadda G (2012) Oxygen activation in flavoprotein oxidases: the importance of being positive. *Biochemistry* **51**, 2662–2669.
- 32 Harreither W, Sygmond C, Augustin M, Narciso M, Rabinovich ML, Gorton L, Haltrich D & Ludwig R (2011) Catalytic properties and classification of cellobiose dehydrogenases from ascomycetes. *Appl Environ Microbiol* **77**, 1804–1815.
- 33 Loose JSM, Forsberg Z, Kracher D, Scheiblbrandner S, Ludwig R, Eijsink VGH & Vaaje-Kolstad G (2016) Activation of bacterial lytic polysaccharide monoxygenases with cellobiose dehydrogenase. *Protein Sci* **25**, 2175–2186.
- 34 Garajova S, Mathieu Y, Beccia MR, Bennati-Granier C, Biaso F, Fanuel M, Ropartz D, Guigliarelli B, Record E, Rogniaux H *et al.* (2016) Single-domain flavoenzymes trigger lytic polysaccharide monoxygenases for oxidative degradation of cellulose. *Sci Rep* **6**, 28276.
- 35 Bissaro B, Forsberg Z, Ni Y, Hollmann F, Vaaje-Kolstad G & Eijsink VGH (2016) Fueling biomass-degrading oxidative enzymes by light-driven water oxidation. *Green Chem* **18**, 5357–5366.
- 36 Kuusk S, Kont R, Kuusk P, Heering A, Sørli M, Bissaro B, Eijsink VGH & Väljamäe P (2019) Kinetic insights into the role of the reductant in H₂O₂-driven degradation of chitin by a bacterial lytic polysaccharide monoxygenase. *J Biol Chem* **294**, 1516–1528.
- 37 Flitsch A, Prasetyo EN, Sygmond C, Ludwig R, Nyanhongo GS & Guebitz GM (2013) Cellulose oxidation and bleaching processes based on recombinant *Myriococcum thermophilum* cellobiose dehydrogenase. *Enzyme Microb Technol* **52**, 60–67.
- 38 Vaaje-Kolstad G, Houston DR, Riemen AHK, Eijsink VGH & Van Aalten DMF (2005) Crystal structure and binding properties of the *Serratia marcescens* chitin-binding protein CBP21. *J Biol Chem* **280**, 11313–11319.
- 39 Sygmond C, Kracher D, Scheiblbrandner S, Zahma K, Felice AKG, Harreither W, Kittl R & Ludwig R (2012) Characterization of the two *Neurospora crassa* cellobiose dehydrogenases and their connection to oxidative cellulose degradation. *Appl Environ Microbiol* **78**, 6161–6171.
- 40 Loose JSM, Forsberg Z, Fraaije MW, Eijsink VGH & Vaaje-Kolstad G (2014) A rapid quantitative activity assay shows that the *Vibrio cholerae* colonization factor GbpA is an active lytic polysaccharide monoxygenase. *FEBS Lett* **588**, 3435–3440.
- 41 Isaksen T, Westereng B, Achmann FL, Agger JW, Kracher D, Kittl R, Ludwig R, Haltrich D, Eijsink VGH & Horn SJ (2014) A C4-oxidizing lytic polysaccharide monoxygenase cleaving both cellulose and cello-oligosaccharides. *J Biol Chem* **289**, 2632–2642.
- 42 Westereng B, Agger JW, Horn SJ, Vaaje-Kolstad G, Achmann FL, Stenstrom YH & Eijsink VGH (2013) Efficient separation of oxidized cello-oligosaccharides generated by cellulose degrading lytic polysaccharide monoxygenases. *J Chromatogr A* **1271**, 144–152.
- 43 Heuts DPHM, Winter RT, Damsma GE, Janssen DB & Fraaije MW (2008) The role of double covalent flavin binding in chito-oligosaccharide oxidase from *Fusarium graminearum*. *Biochem J* **413**, 175–183.